Figure S1 related to figure 1

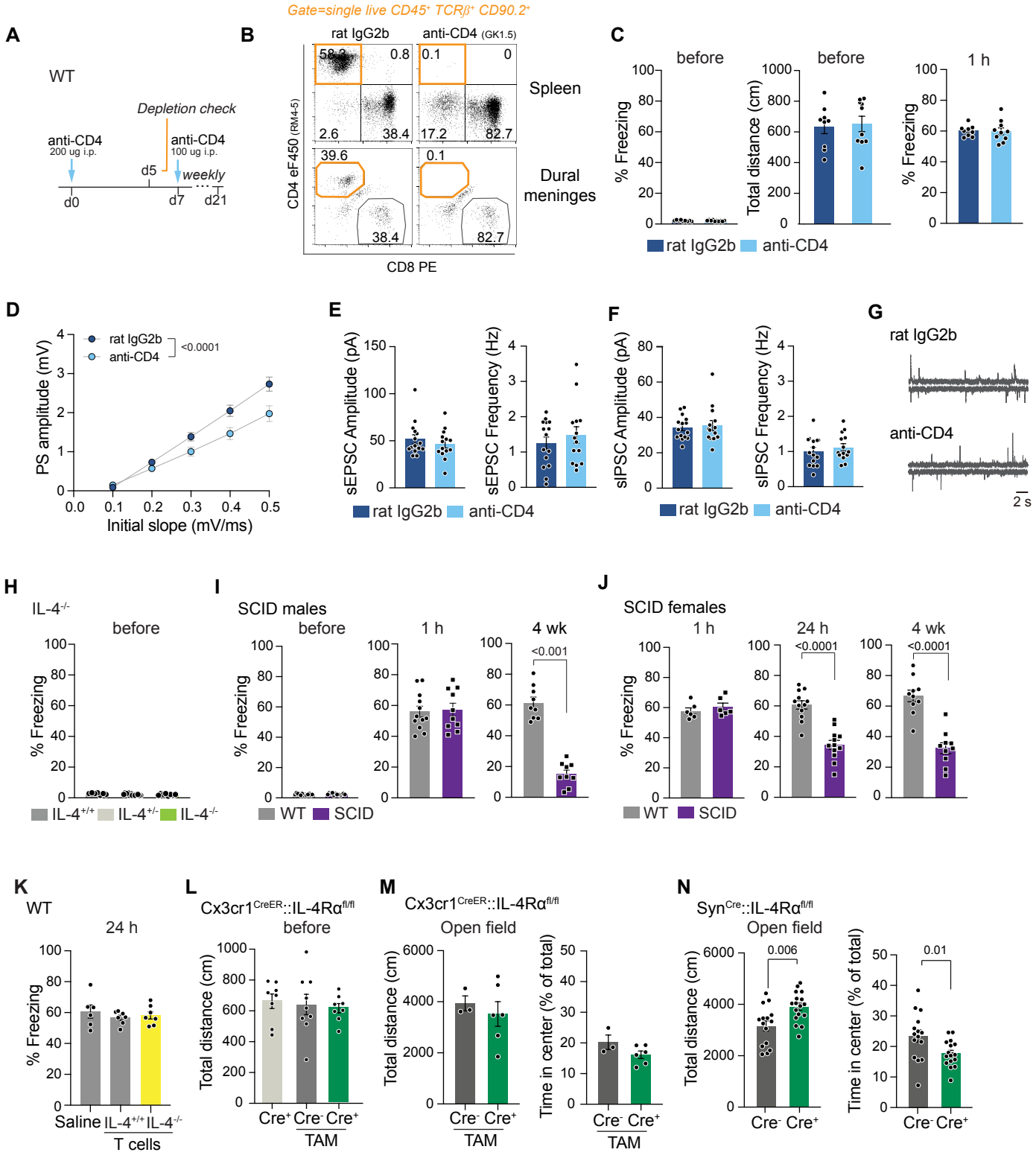

Figure S1. CD4 depleted mice show decreased neuronal excitability but not spontaneous postsynaptic currents. Related to Figure 1.

A, Adult mice were injected with 200 μg CD4 depleting (clone GK1.5) or isotype control antibody (rat IgG2b). Five days after injection, mice were transcardially perfused and CD4 T cell depletion assessed. **B**, Quantification of live $CD45^+$ $TCR\beta^+$ $CD90.2^+$ T cells by flow cytometry showed depletion of CD4 (but not CD8 T cells) in spleen and dural meninges. Representative dot plots of =3 mice per group are shown. **C**, Performance of mice in the CFC paradigm showed no difference in freezing levels and total distance travelled between groups in the context before training and after 1 hour when CD4 T cells were depleted. Data are mean ± SEM, two-tailed unpaired Mann-Whitney *U*-test; n=9 rat IgG2b and n=10 anti-CD4 mice. **D**, Three weeks after CD4 T cell depletion, input-output curves were obtained in the dentate gyrus of the hippocampus. A significant reduction in the stimulus-response relationship and maximal amplitude was determined. Data are presented as mean ± SEM of n=7 rat IgG2b an n=8 anti-CD4 treated mice with 1- 3 slices each. Two-way ANOVA with Bonferroni's multiple comparisons post hoc test. **E - G**, No statistically significant changes in amplitude and frequency of spontaneous excitatory postsynaptic currents (sEPSC**)** (**E**) and amplitude and frequency of spontaneous inhibitory postsynaptic currents (sIPSC) (**F**) were found in the dentate gyrus after CD4 T cell depletion. **G**, Example traces of electrophysiological recordings shown in **E** and **F**. Data are mean ± SEM and 14 - 15 individual neurons shown from n=3 mice per group. Two-tailed unpaired *t*-test. **H**, Quantifications of baseline freezing level during the habituation period in the training box before fear conditioning showing no significant changes between $IL\text{-}4^{+/+}$ (n=7), $IL\text{-}4^{+/-}$ (n=13), $IL\text{-}4^{-/-}$ (n=8) mice. Data are mean ± SEM, one-way ANOVA with Tukey post hoc test. **I, J**, Male (**I**) and female (**J**) wildtype (WT) and SCID mice showed no difference in freezing levels in the context before training and after 1 hour. However, there was a statistically significant difference in SCID mice 24 hours and 4 weeks after training (**I, J and Figure 1F**). Data are mean ± SEM, two-tailed unpaired Mann-Whitney *U*-test, n=13 male WT and n=12 male SCID before, n=12 male WT and n=10 male SCID at 1 hour, n=9 males per group 4 weeks after training; n=6 females 1 hour, n=12 females 24 hours and n=10 females 4 weeks per group after training. **K**, WT mice either injected with saline (n=6) or reconstituted with T cell from $IL\text{-}4^{+/+}$ (n=7) or $IL\text{-}4^{-/-}$ (n=7) showed no significant difference in CFC performance after 24 hours. Data are mean ± SEM, one-way ANOVA with Turkey post hoc test. **L**, The total distance traveled during the

habituation period in the training box before fear conditioning was identical between myeloid cell specific depletion of IL-4Rα (Cx3cr1^{CreER+}::IL-4Rα$^{fl/fl}$) and control groups (Cx3cr1^{CreER-}::IL-4Rα$^{fl/fl}$) after 3 weeks on tamoxifen diet. Data are mean ± SEM, two-tailed unpaired Mann-Whitney *U*-test, n = 8-9 per group. **M**, No differences in total distance traveled and time spend in the center of the open field area were observed in mice with specific depletion of IL-4Rα from macrophages and microglia for 3 weeks n=3 Cre^{-} and n=6 Cre^{+} Cx3cr1^{CreER}::IL-4Rα$^{+/+}$ after 3 weeks on tamoxifen diet per group. Data are mean ± SEM, two-tailed unpaired Mann-Whitney *U*-test, n = 8-9 per group. **N,** Mice specifically depleted of IL-4Rα from neurons showed a significant increase in the distance travelled and decreased time in the center. Data are mean ± SEM, two-tailed unpaired Mann-Whitney *U*-test, n = 15 Syn^{Cre-} and n = 17 Syn^{Cre+} IL-4Rα$^{fl/fl}$ mice, data were pooled from two independent experiments.

Figure S2 related to figure 1

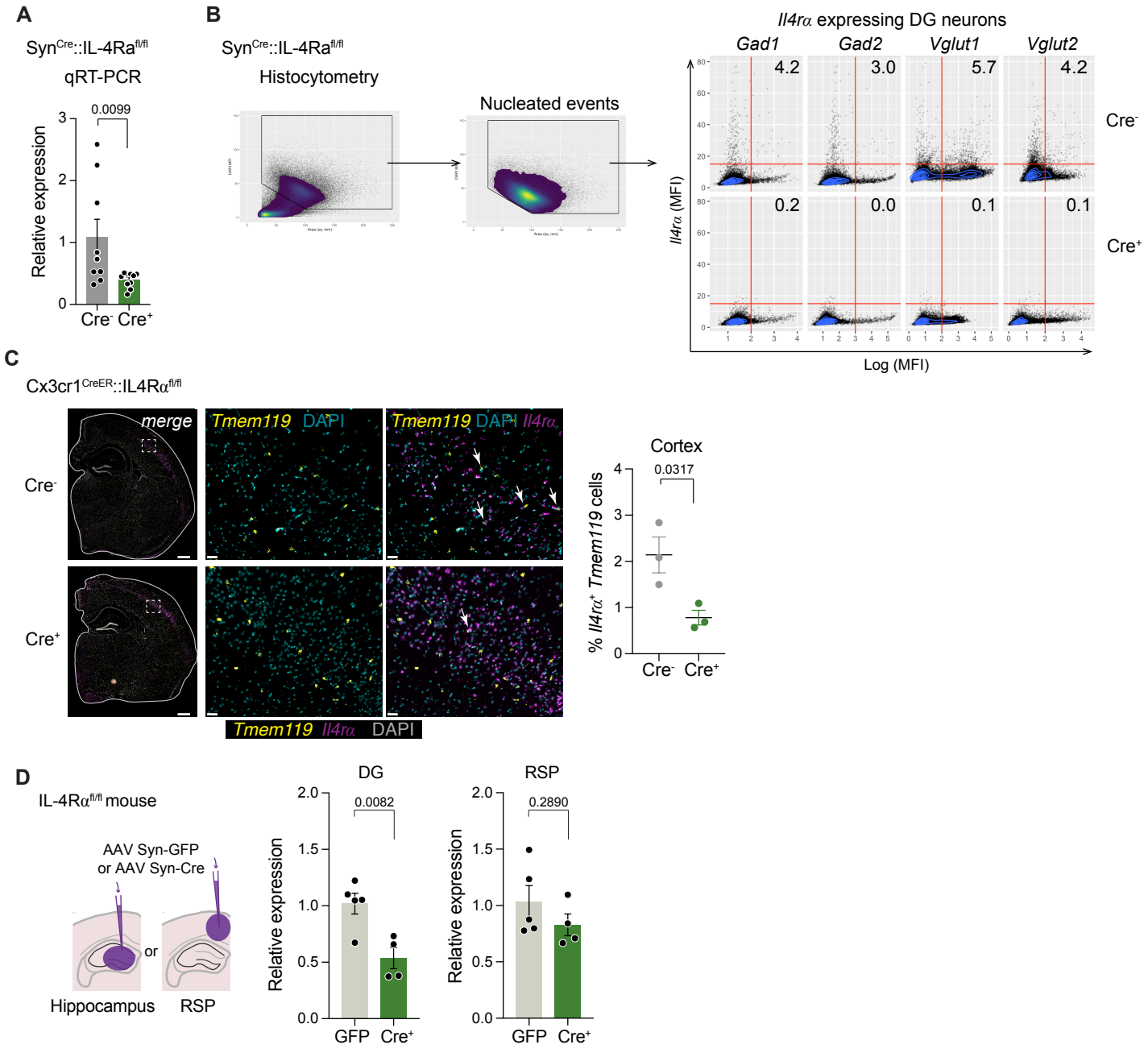

Figure S2. ***Il4rα*** **expression assessment after conditional ablation. Related to Figure 1.**

A, Quantification of *Il4rα* by qRT-PCR in whole hippocampus of Syn^{Cre-}::IL-4R$\alpha^{fl/fl}$ and Syn^{Cre+}::IL-4R$\alpha^{fl/fl}$ mice. Each dot indicates one individual mouse. Data are mean ± SEM, two-tailed unpaired Mann-Whitney *U*-test, n=6 - 7 mice per group. **B,** Quantification of IL-4Rα mRNA expression in inhibitory (*Gad1* and *Gad2*) and excitatory (*Vglut1* and *Vglut2*) neurons of Syn^{Cre-}::IL-4R$\alpha^{fl/fl}$ and Syn^{Cre+}::IL-4R$\alpha^{fl/fl}$ mice by in situ hybridization showed a decreased expression. Each dot indicates one individual neuron. Representative of n=3 mice per group. **C**, Reduction of *Il4rα* expressing microglia in $Cx3cr1^{CreER}$::IL-4R$\alpha^{fl/fl}$ mice after 3 week on tamoxifen diet and two 4-OHT i.p. injections on day 1 and 4 using in situ hybridization with probes for *Il4rα* and microglia (*Tmem119)*. Data are mean ± SEM' two-tailed unpaired *t*-test. **D**, IL-4R$\alpha^{fl/fl}$ mice were injected with AAV Syn-GFP or AAV Syn-Cre-GFP (n=4 - 5 per group) into the RSP or DG. A reduction of receptor expression in cell lysates of micro-dissected dentate gyrus was detected in AAV Syn-Cre-GFP mice by qRT-PCR after 4 weeks. Data are mean ± SEM, two-tailed unpaired Mann-Whitney *U*-test.

Figure S3 related to figure 2

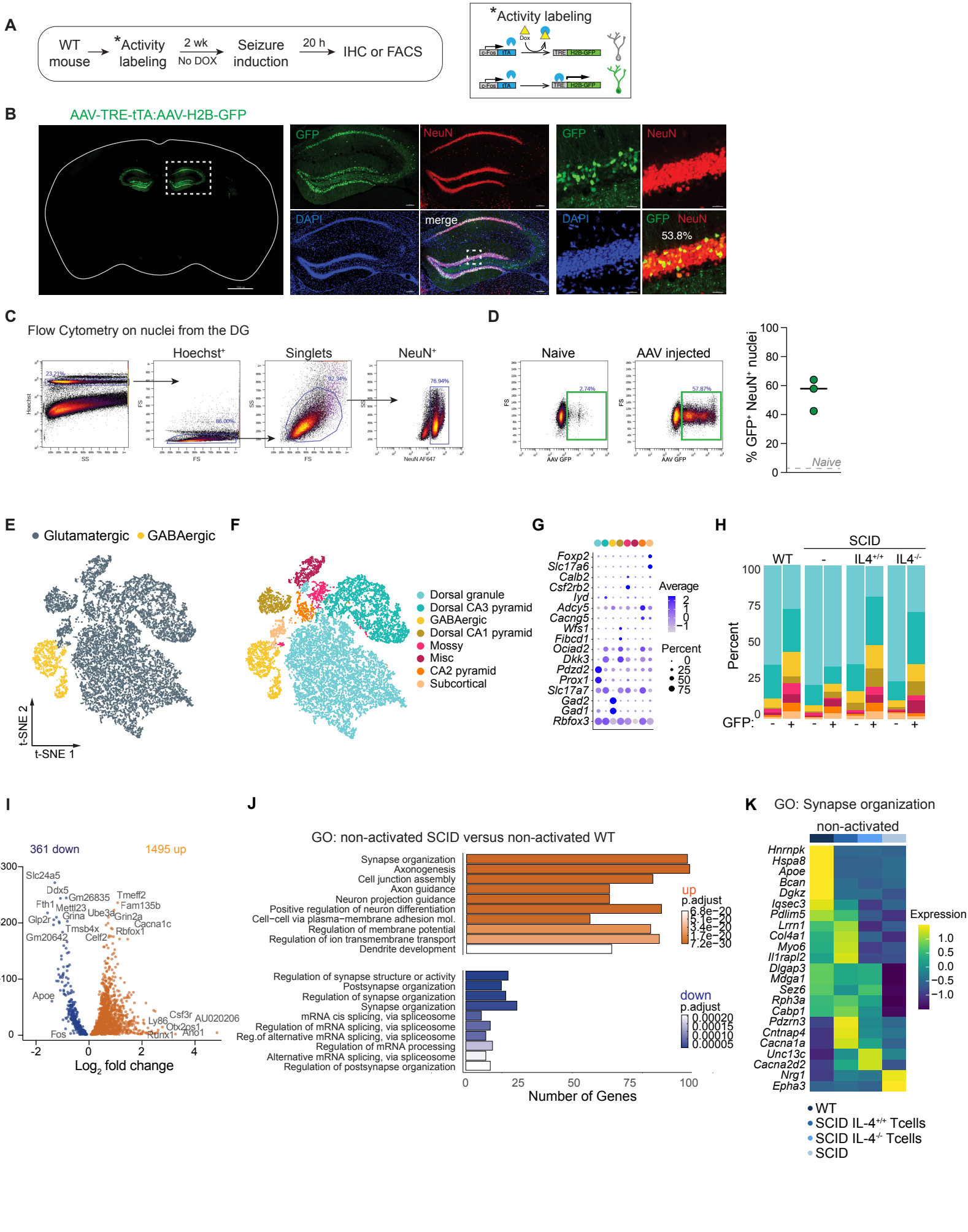

Figure S3. Activity dependent labeling strategy and evaluation of neuronal subtypes in WT, SCID, SCID with T cells in RNAseq dataset. Related to Figure 2.

A, Experimental schematic of neuronal labeling efficiency with virus-based activity labeling method. WT mice were injected with AAV-cFos-tTA and AAV-TRE-H2B-GFP virus in the hippocampus and maintained on normal chow. Two weeks later, mice were injected with kainic acid (25 mg per kilogram) intraperitoneally to induce seizures. **B**, Twenty hours after seizure induction, activated GFP^+ neurons were assessed by immunohistochemistry and GFP^+ $NeuN^+$ neurons found in the dentate gyrus and CA1 region of the hippocampus. Quantifications of the number of GFP^+ and GFP^- $NeuN^+$ neurons in the dorsal dentate gyrus revealed that approximately half of the cells were labelled with AAV-TRE-tTA:AAV-H2B-GFP. Scale bars are 1000 μm, 100 μm or 20 μm. **C, D,** Flow cytometric assessment (**C**) and statistical analysis (**D**) of GFP positive neuronal nuclei after seizure induction determined a labelling efficiency of ~58% (n=3 mice). The protocol was identical to the isolation method for snRNAseq in **Figure 2 and 3**. **E - K**, Neuronal nuclei from the dentate gyrus were obtained from WT or SCID mice, SCID reconstituted with IL-$4^{+/+}$ or IL-$4^{-/-}$ T cells and processed for single cell sequencing. **E**, t-SNE visualization of inhibitory or excitatory neuronal cell types identified. **F,** t-SNE showing clustering of subtypes of neuronal nuclei. **G**, Expression of markers used to identify cell cluster phenotypes. Colors corresponds to the scaled average expression of the genes within each cluster, while size corresponds to the percentage of cells from each cluster showing positive expression of the gene. **H**, Cluster proportions of neuronal subtypes shown in **F**. A lower proportion of the dorsal CA3 pyramid cell cluster in activated GFP^+ SCID neurons was identified when compared to activated GFP^+ WT neurons. Interestingly, adoptive transfer of T cell was sufficient to rescue the deficits in the proportions of cells being activated in SCID mice. **I**, Volcano plot showing differentially expressed genes in non-activated SCID compared to non-activated WT neuronal nuclei. Top differentially expressed genes are labelled with text. **J**, Gene ontology analysis of top 10 pathways by significance comparing differentially expressed genes in non-activated neuronal nuclei from SCID and WT mice. **K**, Heat map showing the average scaled expression of significantly differentially expressed genes in GO:0050808 (synapse organization) between WT, SCID with $IL4^{+/+}$ T cells, SCID with IL-$4^{-/-}$ T cells and SCID of non-activated neuronal nuclei. Mean of n=3-4 biological samples.

Figure S4 related to figure 2

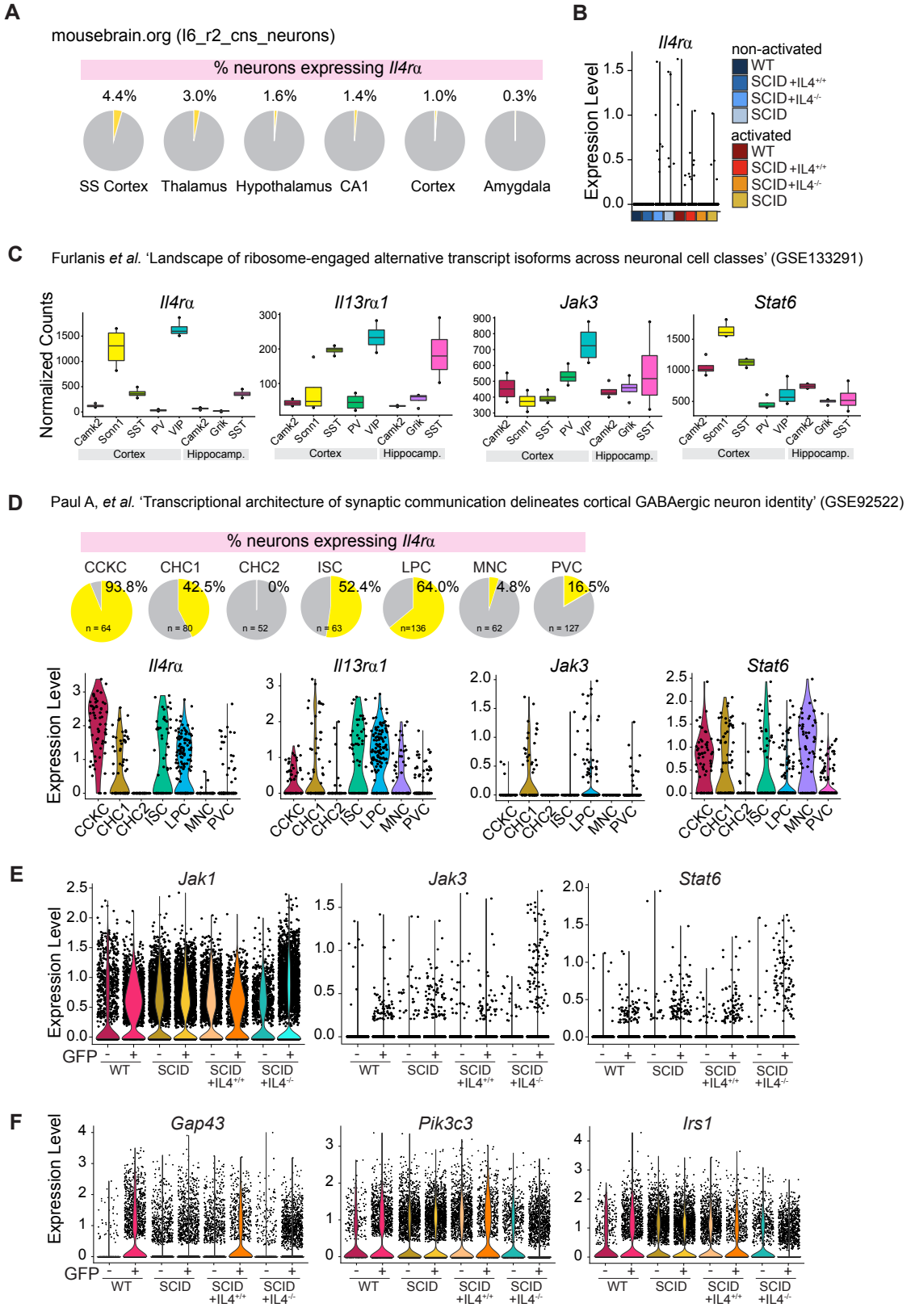

Figure S4. *Il4rα* expression in neurons and effect of task-activation on IL4-mediated signaling in WT, SCID and SCID repopulated with T cells. Related to Figure 2.

A, Expression of *Il4rα* in different brain regions from published RNAseq data sets (mousebrain.org). **B,** *Il4rα* expression in neuronal nuclei from the dentate gyrus of WT, SCID, SCID mice reconstituted with IL-$4^{+/+}$ or IL-$4^{-/-}$ T cells 24 hours after CFC from our snRNAseq data in **Figure 2A-F**. **C**, Expression of *Il4rα, Il13rα1, Jak3* and *Stat6* mRNA in different types of neurons in cortex and hippocampus from published RiboTAG data sets (Furlanis et al., 2019 *Nature Neuroscience*) and **D**, GABAergic neurons in cortical tissue from scRNAseq sets (Paul et al., 2017 *Cell*). **E**, Violin plots demonstrating expression of IL-4Rα signaling molecules *Jak1*, *Jak3* and *Stat6* in non-activated (GFP^-) and activated (GFP^+) in neuronal nuclei from the dentate gyrus of WT, SCID, SCID mice reconstituted with IL-$4^{+/+}$ or IL-$4^{-/-}$ T cells 24 hours after CFC from our snRNAseq data in **Figure 2A-F**. **F**, Signaling of IL-4Rα via the phosphatidylinositol-3 kinase (PI3K) pathway was recently described in neurons [Vogelaar 2018] and *Gap43*, *Pik3c3* and *Irs1* molecules determined in neuronal nuclei.

Figure S5 related to figure 3

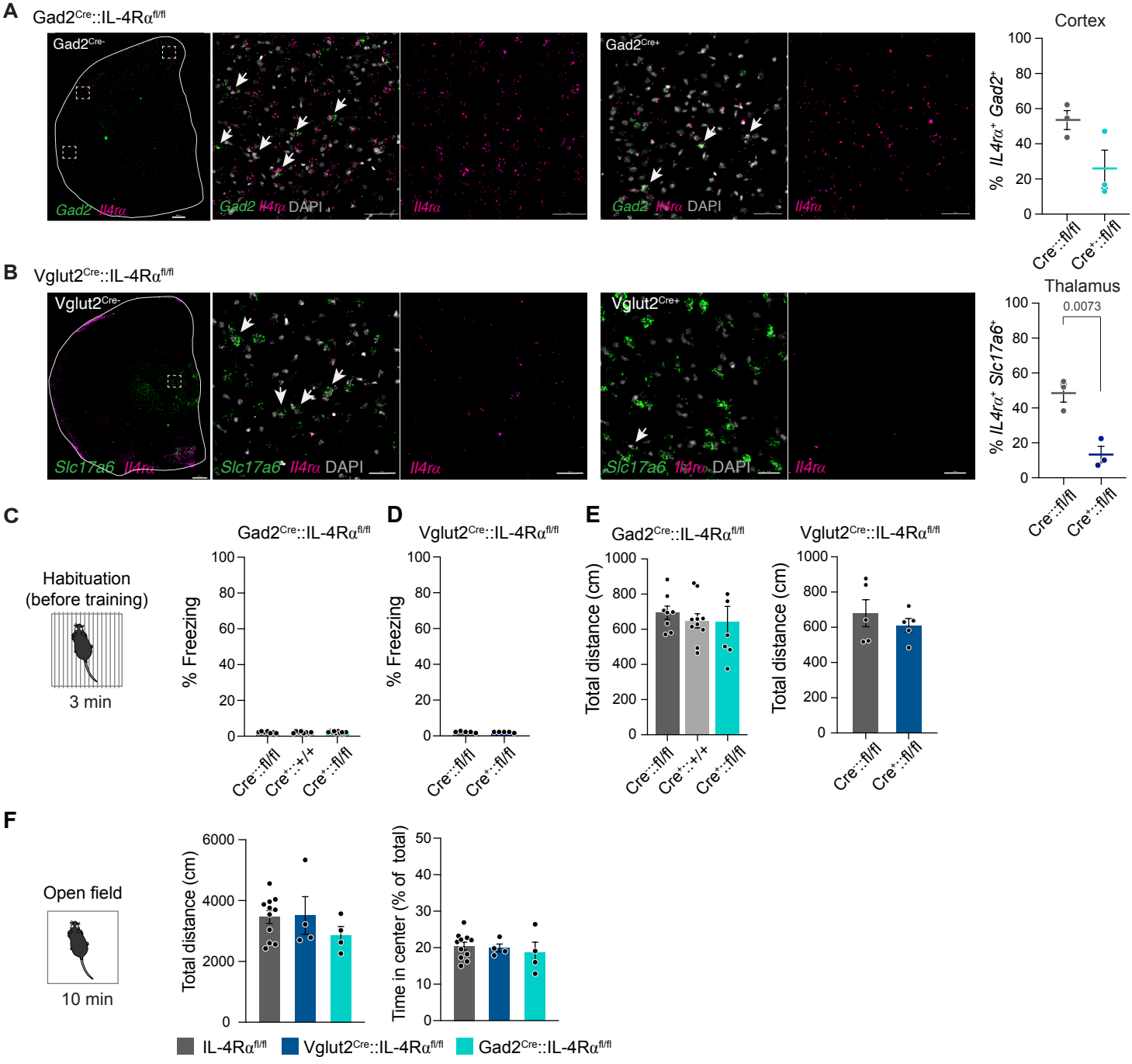

Figure S5. Effect of *Il4rα* depletion in GABAergic and glutamatergic neurons on CFC baseline freezing and open field test. Related to Figure 3.

A, Quantifications of in situ hybridization of Gad2^{Cre}::IL-4Rα$^{fl/fl}$ brain sections showing a notable trend in reduced frequency of IL-4R mRNA expressing inhibitory neurons (*Il4rα*$^{+}$ *Gad2*$^{+}$) in the cortex of Cre^{+} mice compared to Cre^{-} littermates. Scale bar = 100 µm. Data are mean ± SEM, two-tailed unpaired *t*-test, n=3 mice per group; data were pooled from three cortical areas per brain section to obtain enough Gad2^{+} cells. **B,** In situ hybridization of Vglut2^{Cre}::IL-4Rα$^{fl/fl}$ brains showing significantly reduced IL-4R mRNA expression in excitatory (*Il4rα*$^{+}$ *Vglut2*$^{+}$) neurons in the thalamus. Scale bar = 100 µm. Data are mean ± SEM, two-tailed unpaired *t*-test, n=3 mice per group. **C, D**, Quantifications of baseline freezing level during the habituation period in the training box before fear training showing no significant changes between **C**, Cre^{-}:;fl/fl (n=8), Cre^{+}::+/+ (n=10) and Cre^{+}::fl/fl (n=7) Gad2^{Cre}::IL-4Rα$^{fl/fl}$ mice or **D**, Cre^{-}:;fl/fl (n=5) and Cre^{+}:;fl/fl (n=5) Vglut2^{Cre}::IL-4Rα$^{fl/fl}$ mice. **E,** The total distance traveled during the habituation period in the training box before fear conditioning was also identical between mice shown in **C and D.** Data are mean ± SEM, one-way ANOVA with Tukey post hoc test or two-tailed unpaired Mann-Whitney *U*-test. **F**, No differences in total distance traveled and time spend in the center of the open field area were observed in mice with specific depletion of IL-4Rα from glutamatergic and GABAergic mice. IL-4Rα$^{fl/fl}$ (Vglut2^{Cre-} and Gad2^{Cre-}; n=11), Vglut2^{Cre+}::IL-4Rα$^{fl/fl}$ (n=4), Gad2^{Cre+}::IL-4Rα$^{fl/fl}$ (n=4).Data are mean ± SEM, one-way ANOVA with Tukey post hoc test.

Figure S6 related to figure 3

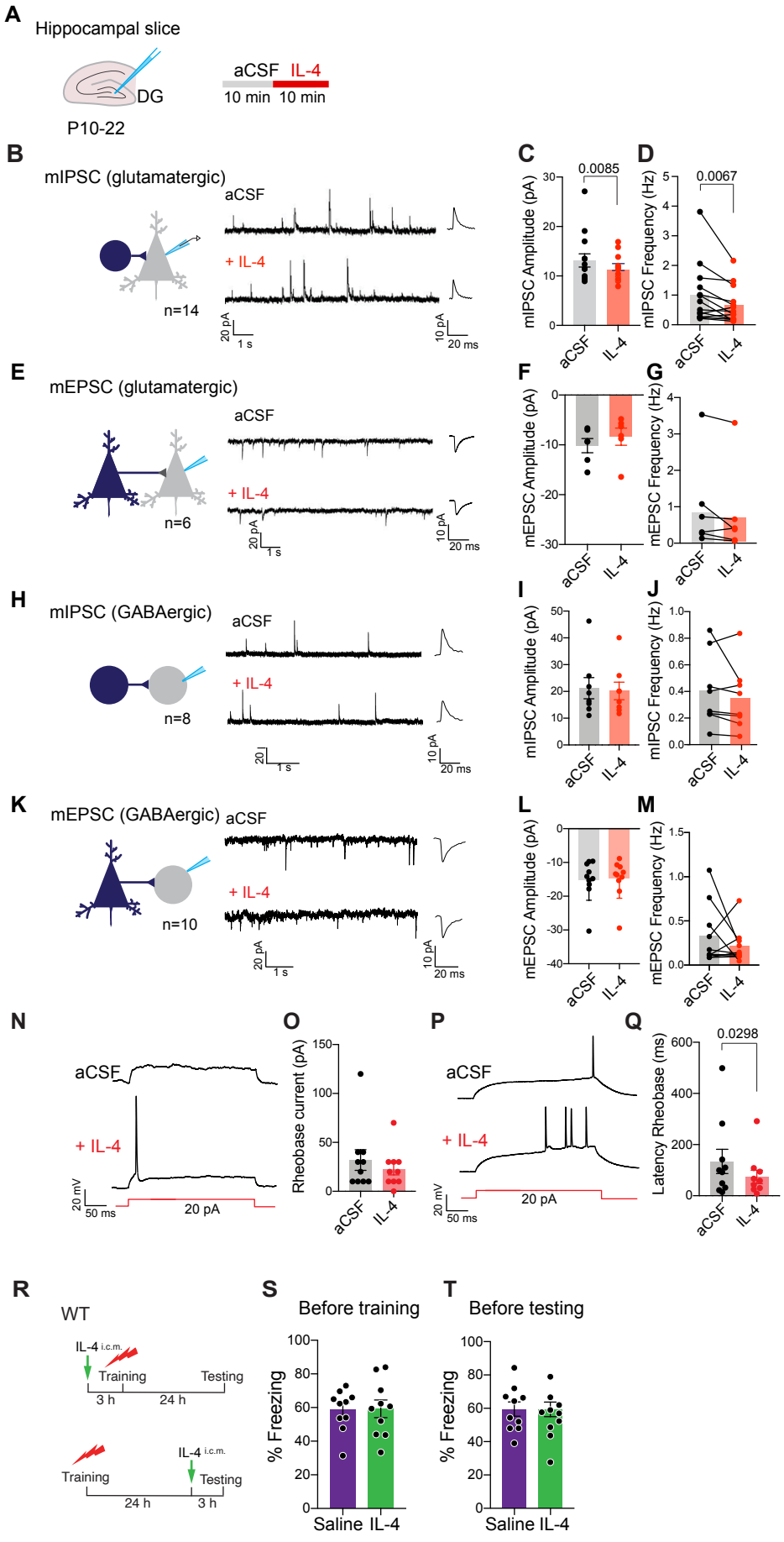

Figure S6. Acute IL-4 treatment of hippocampal slices leads to disinhibition of excitatory neurons. Related to Figure 3.

A, Electrophysiology recording in mIPSC and mEPSC in glutamatergic and GABAergic neurons of the dentate gyrus (DG) during aCSF and 100 ng/ml IL-4 perfusion of postnatal day 10 – 22 C57Bl/6 or Gad2-T2a-NLS-mCherry mice. **B**, Representative electrophysiological recording showing miniature inhibitory post synaptic current (mIPSC) in DG excitatory neurons before and after perfusion with 100 ng/ml IL-4. **C**, Statistical analysis of changes in mIPSC amplitude and **D**, frequency before and after IL-4 perfusion (n=14 neurons from 9 mice). **E**, Example showing miniature excitatory post synaptic current (mEPSC) recording in glutamatergic neurons before and after IL-4 perfusion. **F**, Statistical analysis of changes in mEPSC amplitude and **G,** frequency before and after IL-4 perfusion (n=6 neurons per group). **H**, Recordings showing miniature inhibitory post synaptic current (mIPSC) recording in GABAergic neurons in **I**, amplitude and **J,** frequency before and after IL-4 perfusion (n=8 neurons per group). **K**, Recordings showing miniature excitatory post synaptic current (mEPSC) recording in GABAergic neurons **L**, amplitude and **M,** frequency before and after IL-4 perfusion (n=10 neurons per group). **N**, Examples showing DG excitatory neuronal action potential response upon injection of current during rheobase (the minimum current injection required for action potential) test before and after IL-4 perfusion. **O**, Quantifications of rheobase current before and after IL-4 perfusion. Data are mean ± SEM, two-tailed paired *t*-test; n=10 neurons per group. **P**, Examples showing latency of the response to rheobase in glutamatergic neurons in DG region before and after IL-4 perfusion. **Q**, Quantifications of latency of the response to rheobase in glutamatergic neurons in the DG before and after IL-4 perfusion. Each dot indicates one individual neuron. Data are mean ± SEM, two-tailed paired *t*-test; n=10 neurons per group. **R**, WT mice were injected with saline or 100 units of recombinant IL-4 through intra-cisterna magna (i.c.m.) 3 hours before training or testing. **S**, Percent freezing time of WT mice injected 3 hours before training and **T,** 3 hours before testing was not significantly changed. Each dot indicates one individual mouse, n=10 mice per group. Two-tailed Mann-Whitney *U*-test. Data are presented as mean ± SEM.